
This copy is for your personal, non-commercial use only.

If you wish to distribute this article to others, you can order high-quality copies for your colleagues, clients, or customers by [clicking here](#).

Permission to republish or repurpose articles or portions of articles can be obtained by following the guidelines [here](#).

The following resources related to this article are available online at www.sciencemag.org (this information is current as of April 8, 2011):

Updated information and services, including high-resolution figures, can be found in the online version of this article at:

<http://www.sciencemag.org/content/331/6017/578.full.html>

Supporting Online Material can be found at:

<http://www.sciencemag.org/content/suppl/2011/01/12/science.1197175.DC1.html>

This article **cites 28 articles**, 11 of which can be accessed free:

<http://www.sciencemag.org/content/331/6017/578.full.html#ref-list-1>

This article appears in the following **subject collections**:

Atmospheric Science

<http://www.sciencemag.org/cgi/collection/atmos>

the atmosphere (31, 32). The style of activity imaged requires that the observed slipfaces are not strongly ice-cemented within the erosion depths. Some of the new grainflow alcoves have widths of tens of meters and have recessed in excess of 10 m into the brink. This implies transport of hundreds of cubic meters of sand (fig. S1). Even intermediate-sized gullies such as that in Fig. 5 require movement of tens of cubic meters of sediment.

The reworking of older gully alcoves by aeolian ripples is shown in Fig. 5. The recovery rate of the slipface and the existence of smooth slopes (no grainflows) suggests that grainflow formation and remobilization of sediment by wind may be approximately in equilibrium on a multiyear time scale, although relative rates could vary annually. The seasonal-scale frequency of these two processes demonstrates active sediment transport on polar dunes in the current martian climate. Whether they indicate migration of martian dune forms or simply represent the crestline maintenance of nonmobile dunes can only be determined with future multiyear observations.

In locations where wind energy is insufficient to reconstitute grainflow scars, modification of dune form should ensue. With an estimated sediment transport that delivers tens to hundreds of cubic meters of sand in one Mars year to the dune foot slopes, the initial modification of dune form would be rapid. Resulting dune morphologies would have rounded crests, no brinks, and long, low-angle footslopes. This mechanism may explain some of the unusual dune forms reported on Mars (33). However, because the majority of Mars' north polar dunes do not assume this morphology, we suggest that maintenance of the

dune form is an active process under the current martian climate.

References and Notes

- M. R. Balme, D. Berman, M. Bourke, J. Zimbelman, *Geomorphology* **101**, 703 (2008).
- J. F. McCauley et al., *Icarus* **17**, 289 (1972).
- J. A. Cutts, R. S. U. Smith, *J. Geophys. Res.* **78**, 4139 (1973).
- H. Tsoar, R. Greeley, A. R. Peterfreund, *J. Geophys. Res.* **84** (B14), 8167 (1979).
- A. W. Ward, K. B. Doyle, *Icarus* **55**, 420 (1983).
- M. C. Bourke, K. Edgett, B. Cantor, *Geomorphology* **94**, 247 (2008).
- M. C. Bourke et al., *Proc. Lunar Planet. Sci. Conf.* **40**, 1748 (2009).
- V. Schatz, H. Tsoar, K. S. Edgett, E. J. R. Parteli, H. J. Herrmann, *J. Geophys. Res.* **111** (E4), E002514 (2006).
- In this paper, we use "frost" and "ice" somewhat interchangeably. Martian snow has been shown to increase in density as the winter season progresses (34), so usage of this terminology transitions from one to the other. Readers are encouraged to understand the use of either term to be synonymous with "seasonally condensed volatile."
- M. Malin, K. Edgett, *J. Geophys. Res.* **106** (E10), 23429 (2001).
- C. J. Hansen et al., *Bull. Am. Astron. Soc.* **40**, 409 (2008).
- The numbering of Mars years was defined to facilitate comparison of data sets across decades and multiple Mars missions. Year 1 started 11 April 1955.
- A. McEwen et al., *J. Geophys. Res.* **112** (E5), E002605 (2007).
- A. Kereszturi et al., *Icarus* **201**, 492 (2009).
- A. Kereszturi et al., *Icarus* **207**, 149 (2010).
- D. Möhlmann, A. Kereszturi, *Icarus* **207**, 654 (2010).
- C. Hansen et al., *Proc. Lunar Planet. Sci. Conf.* **41**, 1533 (2010).
- M. C. Malin, K. Edgett, NASA/JPL Planetary Photojournal, <http://photojournal.jpl.nasa.gov/>, catalog no. PIA04290 (2005).
- S. Diniega, S. Byrne, N. T. Bridges, C. M. Dundas, A. S. McEwen, *Geology* **38**, 1047 (2010).
- E. Gardin, P. Allemand, C. Quantin, P. Thollot, *J. Geophys. Res.* **115** (E6), E06016 (2010).
- C. M. Dundas, A. S. McEwen, S. Diniega, S. Byrne, S. Martinez-Alonso, *Geophys. Res. Lett.* **37**, L07202 (2009).
- H. H. Kieffer, Lunar and Planetary Institute contribution 1057 (2000).
- S. Piqueux, P. R. Christensen, *J. Geophys. Res.* **113** (E6), E06005 (2003).
- O. Aharonson, 35th Lunar and Planetary Science Conference, 15 to 19 March 2004, League City, TX, abstr. 1918 (2004).
- H. Kieffer, *J. Geophys. Res.* **112** (E8), E08005 (2007).
- S. Piqueux, P. R. Christensen, *J. Geophys. Res.* **113** (E6), E06005 (2008).
- C. J. Hansen et al., *Icarus* **205**, 283 (2010).
- N. Thomas, C. J. Hansen, G. Portyankina, P. S. Russell, *Icarus* **205**, 296 (2010).
- G. Portyankina, W. J. Markiewicz, N. Thomas, C. J. Hansen, M. Milazzo, *Icarus* **205**, 311 (2010).
- S. Silvestro et al., *Second International Dunes Conference, LPI Contributions*, **1552**, 65 (2010).
- M. Mellon et al., *J. Geophys. Res.* **114**, E00E07 (2009).
- N. Putzig et al., *Proc. Lunar Planet. Sci. Conf.* **41**, 1533 (2010).
- R. Hayward et al., *J. Geophys. Res.* **112** (E11), E11007 (2007).
- K. Matsuo, K. Heki, *Icarus* **202**, 90 (2009).
- L_s is the true anomaly of Mars in its orbit around the sun, measured from the martian vernal equinox, used as a measure of the season on Mars. $L_s = 0$ corresponds to the beginning of northern spring; $L_s = 180$ is the beginning of southern spring.
- This work was partially supported by the Jet Propulsion Laboratory, California Institute of Technology, under a contract with NASA.

Supporting Online Material

www.sciencemag.org/cgi/content/full/331/6017/575/DC1

SOM Text

Fig. S1

References

10 September 2010; accepted 10 January 2011
10.1126/science.1197636

2500 Years of European Climate Variability and Human Susceptibility

Ulf Büntgen,^{1,2*} Willy Tegel,³ Kurt Nicolussi,⁴ Michael McCormick,⁵ David Frank,^{1,2} Valerie Trouet,^{1,6} Jed O. Kaplan,⁷ Franz Herzig,⁸ Karl-Uwe Heussner,⁹ Heinz Wanner,² Jürg Luterbacher,¹⁰ Jan Esper¹¹

Climate variations influenced the agricultural productivity, health risk, and conflict level of preindustrial societies. Discrimination between environmental and anthropogenic impacts on past civilizations, however, remains difficult because of the paucity of high-resolution paleoclimatic evidence. We present tree ring–based reconstructions of central European summer precipitation and temperature variability over the past 2500 years. Recent warming is unprecedented, but modern hydroclimatic variations may have at times been exceeded in magnitude and duration. Wet and warm summers occurred during periods of Roman and medieval prosperity. Increased climate variability from ~250 to 600 C.E. coincided with the demise of the western Roman Empire and the turmoil of the Migration Period. Such historical data may provide a basis for counteracting the recent political and fiscal reluctance to mitigate projected climate change.

Continuing global warming and its potential associated threats to ecosystems and human health present a substantial challenge to modern civilizations that already experience many direct and indirect impacts of anthropogenic climate change (1–4). The rise and fall of

past civilizations have been associated with environmental change, mainly due to effects on water supply and agricultural productivity (5–9), human health (10), and civil conflict (11). Although many lines of evidence now point to climate forcing as one agent of distinct episodes of societal

crisis, linking environmental variability to human history is still limited by the dearth of high-resolution paleoclimatic data for periods earlier than 1000 years ago (12).

Archaeologists have developed oak (*Quercus* spp.) ring width chronologies from central Europe that cover nearly the entire Holocene and have used them for the purpose of dating archaeological artifacts, historical buildings, antique artwork, and furniture (13). The number of samples contributing to these records fluctuates between hundreds

¹Swiss Federal Research Institute for Forest, Snow and Landscape Research (WSL), 8903 Birmensdorf, Switzerland. ²Oeschger Centre for Climate Change Research, University of Bern, 3012 Bern, Switzerland. ³Institute for Forest Growth, University of Freiburg, 79085 Freiburg, Germany. ⁴Institute of Geography, University of Innsbruck, 6020 Innsbruck, Austria. ⁵Department of History, Harvard University, Cambridge, MA 02138, USA. ⁶Laboratory of Tree-Ring Research, University of Arizona, Tucson, AZ 85721, USA. ⁷Environmental Engineering Institute, École Polytechnique Fédérale de Lausanne, 1015 Lausanne, Switzerland. ⁸Bavarian State Department for Cultural Heritage, 86672 Thierhaupten, Germany. ⁹German Archaeological Institute, 14195 Berlin, Germany. ¹⁰Department of Geography, Justus Liebig University, 35390 Giessen, Germany. ¹¹Department of Geography, Johannes Gutenberg University, 55128 Mainz, Germany.

*To whom correspondence should be addressed. E-mail: buentgen@wsl.ch

and thousands in periods of societal prosperity, whereas fewer samples from periods of socioeconomic instability are available (14). Chronologies of living (15) and relict oaks (16, 17) may reflect distinct patterns of summer precipitation and drought if site ecology and local climatology imply moisture deficits during the vegetation period. Annually resolved climate reconstructions that contain long-term trends and extend prior to medieval times, however, depend not only on the inclusion of numerous ancient tree-ring samples of sufficient climate sensitivity, but also on frequency preservation, proxy calibration, and uncertainty estimation (18–20).

To better understand interannual to multicentennial changes in central European April-to-June (AMJ) precipitation over the late Holocene, we used 7284 precipitation-sensitive oak ring width series from subfossil, archaeological, historical, and recent material representing temperate forests in northeastern France (NEF), northeastern Germany (NEG), and southeastern Germany (SEG) (Fig. 1). We found that the mean annual replication was 286 series, with a maximum of 550 series during Roman times and the smallest sample size of 44 series at ~400 C.E. Growth variations among the three regions were significantly ($P < 0.001$) correlated over the past two millennia: NEF/SEG at 0.53, SEG/NEG at 0.47, and NEF/NEG at 0.37 (21). Correlation coefficients among AMJ precipitation readings from three stations in NEF, NEG, and SEG averaged 0.31 over the common instrumental

period (1921 to 1988), whereas the three regional oak chronologies correlated at 0.37 over the same interval (21).

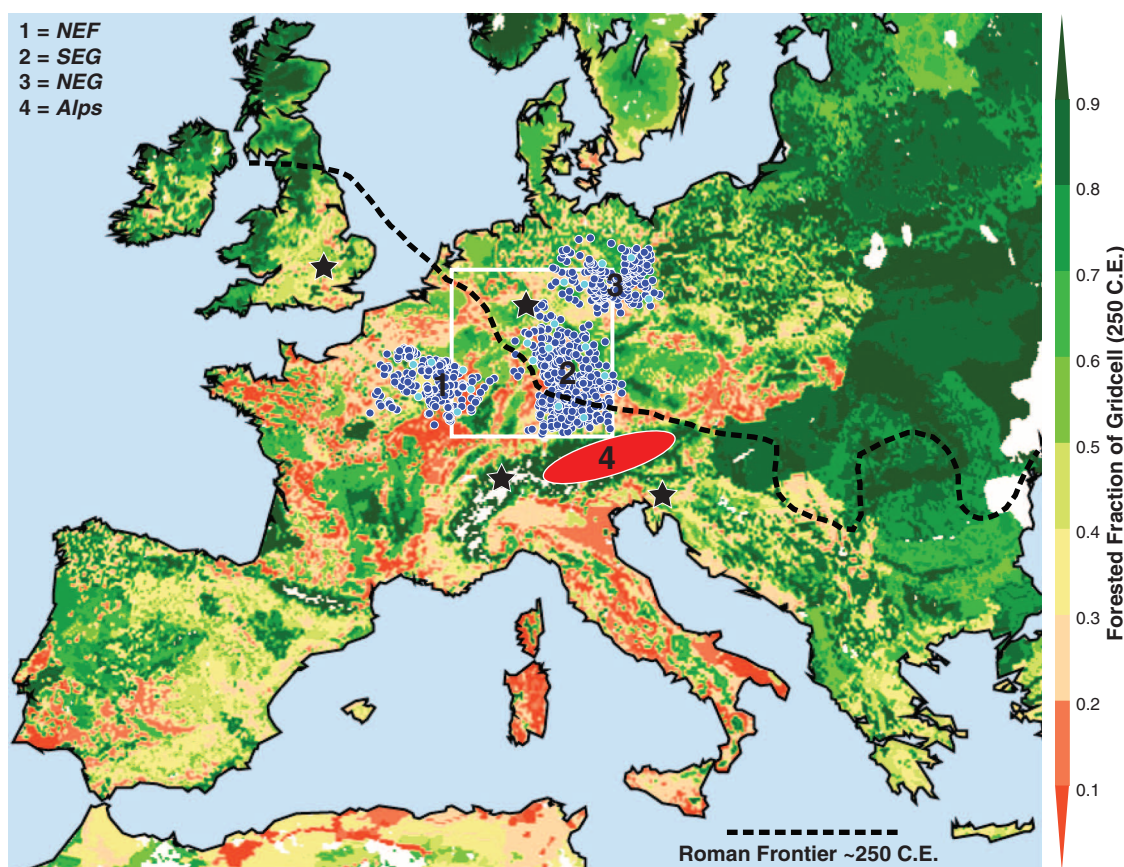
The temporal distribution of historical tree harvest (i.e., felling dates) mimics preindustrial deforestation and population trends (Fig. 2), implying substantial anthropogenic landscape perturbation over the last 2500 years (22). Increased felling dates reflect construction activity during the late Iron Age and Roman Empire (~300 B.C.E. to 200 C.E.) and indicate that the maximum expansion and deforestation of the Western Roman Empire (WRE) occurred around 250 C.E. Reduced tree harvesting at ~250 to 400 C.E. coincides with the biggest central European historical crisis, the Migration Period, a time marked by lasting political turmoil, cultural change, and socioeconomic instability (23, 24). Increasing timber harvest for construction is represented by abundant felling parallel to socioeconomic consolidation from the 6th to the 9th centuries C.E. Many earlier structures were replaced during a settlement boom in the 13th century (23, 24), eliminating much construction evidence from the central medieval period (900 to 1100 C.E.). Construction activity during the last millennium was disrupted by the Great Famine and Black Death (19) as well as by the Thirty Years' War.

To assess climatic drivers of oak growth during industrial and preindustrial times, we compared chronologies of high-frequency variability

with instrumental records, independent climate reconstructions, and historical archives (21). A total of 87 different medieval written sources comprise 88 eyewitness accounts of regional hydroclimatic conditions (with as many as seven reports per year) resolved to the year or better, which corroborate 30 out of 32 of the extremes preserved in our oak record between 1013 and 1504 C.E., whereas 16 reports were found to be contradictory (Fig. 3A). These observations further confirm the spatial signature of the climatic signal reflected by the oak network. Scaled precipitation anomaly composites calculated for the 12 most positive and the 16 most negative oak extremes back to 1500 C.E. revealed significantly wet and dry central European summers, respectively (Fig. 3B) (21). Independently derived extremes in pan-European oak growth over the last millennium match 5 of 11 extremes at the central European network level, and 21 of 53 at the regional scale (fig. S6).

The regional oak chronologies correlate on average at 0.39 with AMJ precipitation variability (1901–1980) averaged over 45° to 50°N and 8° to 10°E. Increased agreement between the tree-ring proxy and instrumental target records is obtained from the combined central European oak record, which correlates at 0.50 to 0.59 with interannual to multidecadal variations in AMJ precipitation (fig. S9). Correlation between this study and an independent summer drought reconstruction from central Germany (19) is 0.56

Fig. 1. Location of the 7284 central European oak samples (blue) and the network of 1546 Alpine conifers (red), superimposed on a deforestation model of Roman land use and land cover around 250 C.E. (22). Black stars indicate the location of the independent tree-ring chronologies used for comparison (16–19); the white box denotes the area over which gridded precipitation totals were averaged and used for proxy calibration.



over the common 996 to 2005 C.E. period (Fig. 4). To complement our hydroclimatic reconstruction, we also developed a central European summer temperature proxy based on 1089 stone pine (*Pinus cembra*) and 457 European larch (*Larix decidua*) ring width series from high-elevation sites in the Austrian Alps and adjacent areas (21). This composite record includes living trees, historical timber, and subfossil wood, and correlates at 0.72 to 0.92 with interannual to multidecadal variations in instrumental June-to-August (JJA) temperature (1864–2003). The new proxy is significantly positive correlated with 20th century JJA temperatures of central Europe and the Mediterranean region (21), and possesses high- to low-frequency agreement with an independent maximum latewood density-based temperature surrogate from the Swiss Alps (18) ($r = 0.35$ to 0.44 ; 755 to 2003 C.E.) (Fig. 4).

AMJ precipitation was generally above average and fluctuated within fairly narrow margins from the Late Iron Age through most of the Roman Period until ~250 C.E., whereas two depressions in JJA temperature coincided with the Celtic Expansion (~350 B.C.E.) and the Roman Conquest (~50 B.C.E.). Exceptional climate variability is reconstructed for ~250 to 550 C.E. and coincides with some of the most severe chal-

lenges in Europe's political, social, and economic history, during the Migration Period. Distinct drying in the 3rd century paralleled a period of serious crisis in the WRE marked by barbarian invasion, political turmoil, and economic dislocation in several provinces of Gaul, including Belgica, Germania superior, and Rhaetia (24, 25). Precipitation increased during the recovery of the WRE in the 300s under the dynasties of Constantine and Valentinian, while temperatures were below average. Precipitation surpassed early imperial levels during the demise of the WRE in the 5th century before dropping sharply in the first half of the 6th century. At the same time, falling lake levels in Europe and Africa (1, 26) accompanied hemispheric-scale cooling that has been linked with an explosive near-equatorial volcanic eruption in 536 C.E. (27), followed by the first pandemic of Justinian plague that spread from the eastern Mediterranean in 542–543 C.E. (28). Rapid climate changes together with frequent epidemics had the overall capacity to disrupt the food production of agrarian societies (5–8). Most of the oak samples from this period originate from archaeological excavations of water wells and subfossil remains currently located in floodplains and wetlands (Fig. 2D), possibly attesting to drier conditions during their colonization.

AMJ precipitation and JJA temperature began to increase from the end of the 6th century C.E. and reached climate conditions comparable to those of the Roman period in the early 800s. The onset of wetter and warmer summers is contemporaneous with the societal consolidation of new kingdoms that developed in the former WRE (23). Reduced climate variability from ~700 to 1000 C.E., relative to its surroundings, matches the new and sustained demographic growth in the northwest European countryside, and even the establishment of Norse colonies in the cold environments of Iceland and Greenland (9). Humid and mild summers paralleled the rapid cultural and political growth of medieval Europe under the Merovingian and Carolingian dynasties and their successors (23). Average precipitation and temperature showed fewer fluctuations during the period of peak medieval demographic and economic growth, ~1000 to 1200 C.E. (22, 23). Wetter summers during the 13th and 14th centuries and a first cold spell at ~1300 C.E. agree with the globally observed onset of the Little Ice Age (20, 29), likely contributing to widespread famine across central Europe. Unfavorable climate may have even played a role in debilitating the underlying health conditions that contributed to the

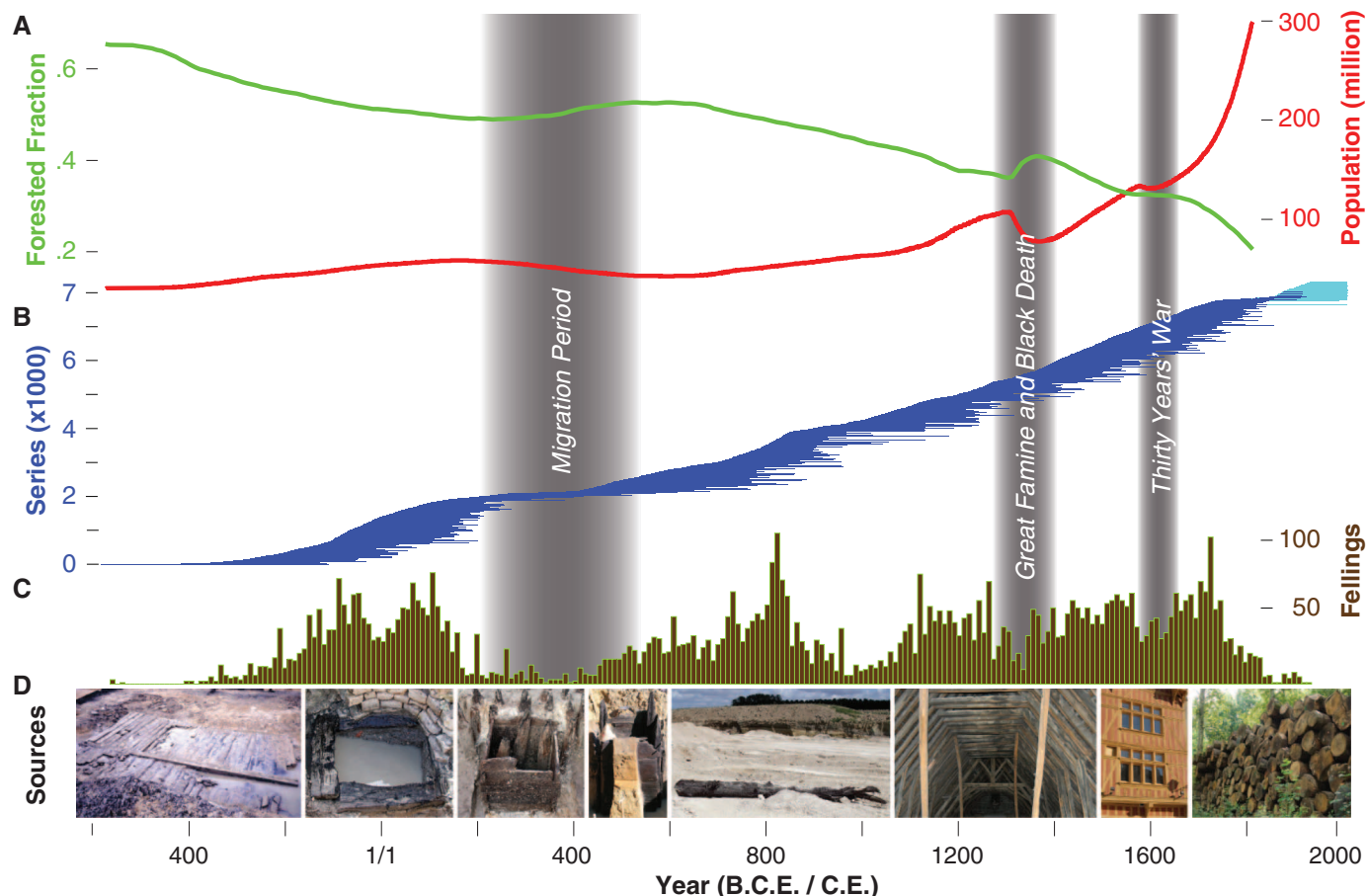


Fig. 2. (A to D) Evolution of central European forest cover and population from (22) (A), together with oak sample replication (B), their historical end dates at decadal resolution (C), and examples of archaeological (left), subfossil, historical, and recent (right) sample sources (D).

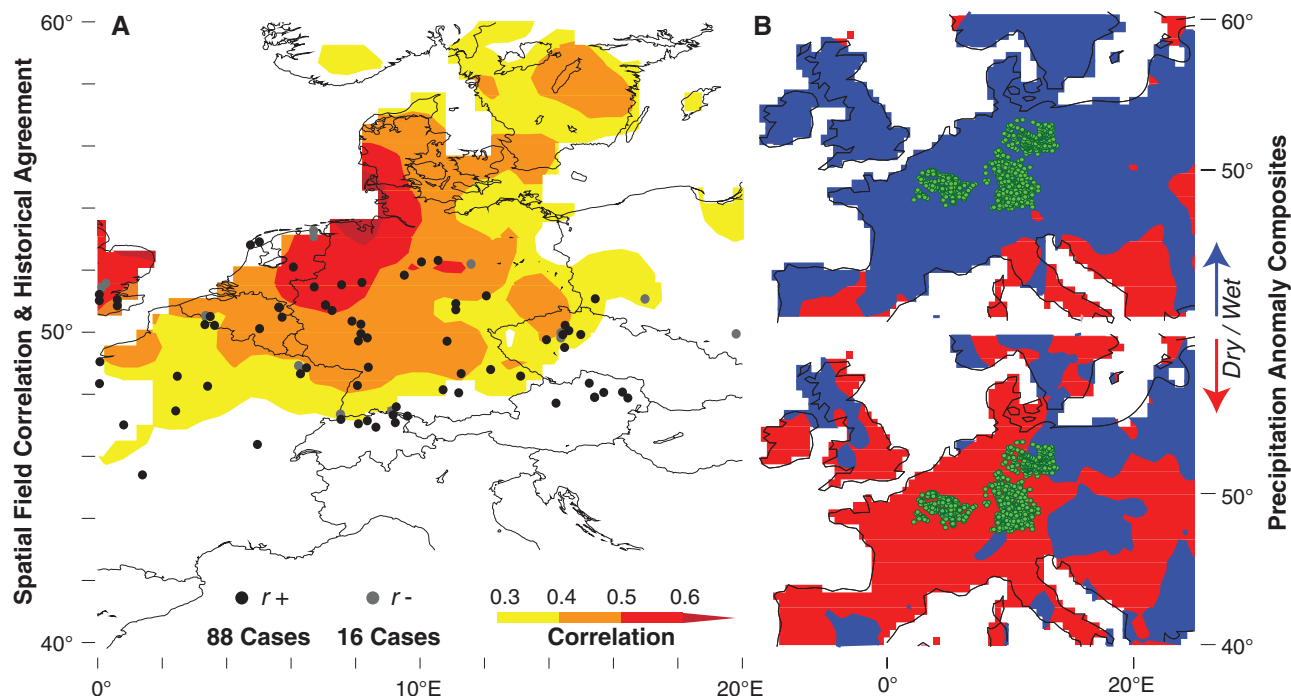


Fig. 3. (A) Correlation map of the mean oak chronology against gridded central European AMJ precipitation data (1901–1980) together with the location of 104 historical reports, of which 88 witnesses corroborate 30 of 32 climatic extremes that were reconstructed from the oak data between 1013 and 1504, whereas 16 witnesses offer contradictory reports. Note that different reports may originate from the same location. (B) Composite anomaly fields (scaled means, modified

t values) of summer (JJA) precipitation computed for 12 positive (top) and 16 negative (bottom) oak extremes between 1500 and 2000 (21). Significance of the composite anomalies, relative to the 1901–2000 climatology, was computed using 95% confidence thresholds of the modified two-sided t test (21). Blue and red colors refer to significantly wet and dry conditions, respectively. Green dots refer to the location of 7284 central European oak samples.

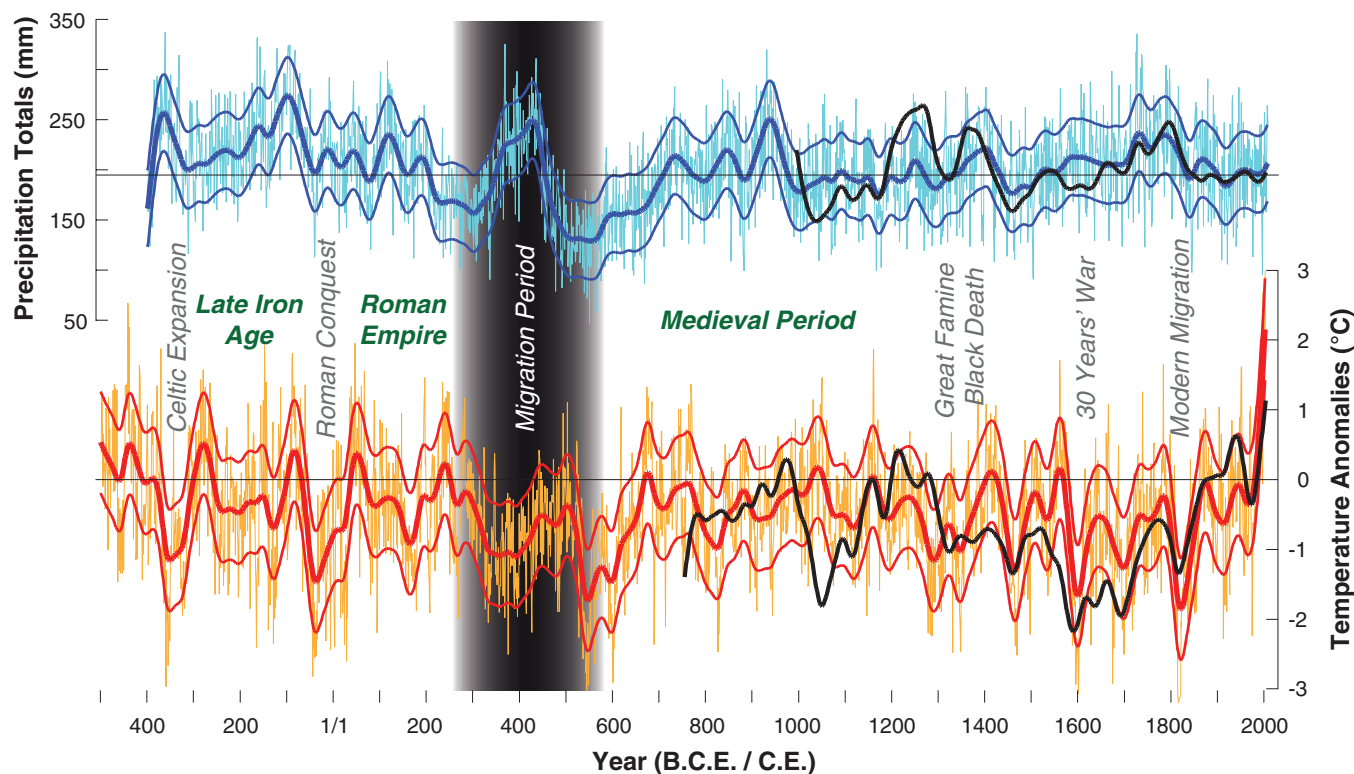


Fig. 4. Reconstructed AMJ precipitation totals (top) and JJA temperature anomalies (bottom) with respect to the 1901–2000 period. Error bars are ± 1 RMSE of the calibration periods. Black lines show independent precipitation and temperature reconstructions from Germany (19) and

Switzerland (18). Bold lines are 60-year low-pass filters. Periods of demographic expansion, economic prosperity, and societal stability are noted, as are periods of political turmoil, cultural change, and population instability.

devastating economic crisis that arose from the second plague pandemic, the Black Death, which reduced the central European population after 1347 C.E. by 40 to 60% (19, 22, 28). The period is also associated with a temperature decline in the North Atlantic and the abrupt desertion of former Greenland settlements (9). Temperature minima in the early 17th and 19th centuries accompanied sustained settlement abandonment during the Thirty Years' War and the modern migrations from Europe to America.

The rate of natural precipitation and temperature change during the Migration Period may represent a natural analog to rates of projected anthropogenic climate change. Although modern populations are potentially less vulnerable to climatic fluctuations than past societies have been, they also are certainly not immune to the predicted temperature and precipitation changes, especially considering that migration to more favorable habitats (22) as an adaptive response will not be an option in an increasingly crowded world (6). Comparison of climate variability and human history, however, prohibits any simple causal determination; other contributing factors such as sociocultural stressors must be considered in this complex interplay (7, 30). Nonetheless, the new climate evidence sets a paleoclimatic benchmark in terms of temporal resolution, sample replication, and record length.

Our data provide independent evidence that agrarian wealth and overall economic growth might be related to climate change on high- to mid-frequency (interannual to decadal) time scales. Preindustrial societies were sensitive to famine, disease, and war, which were often driven by drought, flood, frost or fire events, as independently described by documentary archives (30).

It also appears to be likely that societies can better compensate for abrupt (annual) climatic extremes and have the capacity to adapt to slower (multidecadal to centennial) environmental changes (6, 7).

The historical association of precipitation and temperature variation with population migration and settlement desertion in Europe may provide a basis for questioning the recent political and fiscal reluctance to mitigate projected global climate change (31), which reflects the common societal belief that civilizations are insulated from variations in the natural environment.

References and Notes

1. T. M. Shanahan *et al.*, *Science* **324**, 377 (2009).
2. E. R. Cook, R. Seager, M. A. Cane, D. W. Stahle, *Earth Sci. Rev.* **81**, 93 (2007).
3. M. E. Mann, J. D. Woodruff, J. P. Donnelly, Z. Zhang, *Nature* **460**, 880 (2009).
4. E. R. Cook *et al.*, *Science* **328**, 486 (2010).
5. B. M. Buckley *et al.*, *Proc. Natl. Acad. Sci. U.S.A.* **107**, 6748 (2010).
6. H. Weiss, R. S. Bradley, *Science* **291**, 609 (2001).
7. P. B. deMenocal, *Science* **292**, 667 (2001).
8. G. H. Haug *et al.*, *Science* **299**, 1731 (2003).
9. W. P. Patterson, K. A. Dietrich, C. Holmden, J. T. Andrews, *Proc. Natl. Acad. Sci. U.S.A.* **107**, 5306 (2010).
10. A. J. McMichael, R. E. Woodruff, S. Hales, *Lancet* **367**, 859 (2006).
11. M. B. Burke, E. Miguel, S. Satyanath, J. A. Dykema, D. B. Lobell, *Proc. Natl. Acad. Sci. U.S.A.* **106**, 20670 (2009).
12. P. D. Jones *et al.*, *Holocene* **19**, 3 (2009).
13. K. Haneca, K. Ćufar, H. Beekman, *J. Archaeol. Sci.* **36**, 1 (2009).
14. W. Tegel, J. Vanmoerkerke, U. Büntgen, *Quat. Sci. Rev.* **29**, 1957 (2010).
15. D. A. Friedrichs *et al.*, *Tree Physiol.* **29**, 39 (2009).
16. P. M. Kelly, H. H. Leuschner, K. R. Briffa, I. C. Harris, *Holocene* **12**, 689 (2002).
17. K. Ćufar, M. De Luis, D. Eckstein, L. Kajfez-Bogataj, *Int. J. Biometeorol.* **52**, 607 (2008).
18. U. Büntgen, D. C. Frank, D. Nievergelt, J. Esper, *J. Clim.* **19**, 5606 (2006).
19. U. Büntgen *et al.*, *Quat. Sci. Rev.* **29**, 1005 (2010).
20. D. C. Frank *et al.*, *Nature* **463**, 527 (2010).
21. See supporting material on Science Online.
22. J. O. Kaplan, K. M. Krumhardt, N. Zimmermann, *Quat. Sci. Rev.* **28**, 3016 (2009).
23. M. McCormick, *Origins of the European Economy: Communications and Commerce, A.D. 300–900* (Cambridge Univ. Press, Cambridge, 2001).
24. R. Duncan-Jones, in *Approaching Late Antiquity: The Transformation from Early to Late Empire*, S. Swain, M. Edwards, Eds. (Oxford Univ. Press, Oxford, 2004), pp. 20–52.
25. C. Witschel, *J. Roman Archaeol.* **17**, 251 (2004).
26. D. J. Charman, A. Blundell, R. C. Chiverrell, D. Hendon, P. G. Langdon, *Quat. Sci. Rev.* **25**, 336 (2006).
27. L. B. Larsen *et al.*, *Geophys. Res. Lett.* **35**, L04708 (2008).
28. K. L. Kausrud *et al.*, *BMC Biol.* **8**, 112 (2010).
29. V. Trouet *et al.*, *Science* **324**, 78 (2009).
30. R. Brázdil, C. Pfister, H. Wanner, H. von Storch, J. Luterbacher, *Clim. Change* **70**, 363 (2005).
31. D. B. Lobell *et al.*, *Science* **319**, 607 (2008).
32. We thank E. Cook, K. Gibson, G. Haug, G. Huang, D. Johnson, M. Küttel, N. Stenseth, E. Zorita, and two anonymous referees for comments and discussion. Supported by the Swiss National Science Foundation (NCCR-Climate), the Deutsche Forschungsgemeinschaft projects PRIME (62201185) and Paleoclimatology of the Middle East (62201236), the Austrian Science Fund FWF (P15828, F3113-G02), l'Institut National de Recherches Archéologiques Préventives, the Andrew W. Mellon Foundation, and European Union projects MILLENNIUM (017008), ACQWA (212250), and CIRCE (036961).

Supporting Online Material

www.sciencemag.org/cgi/content/full/science.1197175/DC1
Materials and Methods
Figs. S1 to S12
Tables S1 and S2
References

31 August 2010; accepted 5 January 2011
Published online 13 January 2011;
10.1126/science.1197175

Passive Origins of Stomatal Control in Vascular Plants

Tim J. Brodribb* and Scott A. M. McAdam

Carbon and water flow between plants and the atmosphere is regulated by the opening and closing of minute stomatal pores in surfaces of leaves. By changing the aperture of stomata, plants regulate water loss and photosynthetic carbon gain in response to many environmental stimuli, but stomatal movements cannot yet be reliably predicted. We found that the complexity that characterizes stomatal control in seed plants is absent in early-diverging vascular plant lineages. Lycophte and fern stomata are shown to lack key responses to abscisic acid and epidermal cell turgor, making their behavior highly predictable. These results indicate that a fundamental transition from passive to active metabolic control of plant water balance occurred after the divergence of ferns about 360 million years ago.

The evolution of stomata at least 400 million years ago (1) enabled plants to transform their epidermis into a dynamically permeable layer that could be either water-tight under dry conditions or highly permeable to

photosynthetic CO₂ during favorable conditions. The combination of adjustable stomata with an internal water transport system was a turning point in plant evolution that enabled vascular plants to invade most terrestrial environments

(2). Today, the leaves of vascular plants possess arrays of densely packed stomata, each one comprising a pair of adjacent guard cells (Fig. 1). High turgor pressure deforms the guard cells to form an open pore, which allows rapid diffusion of atmospheric CO₂ through the epidermis into the photosynthetic tissues inside the leaf. Declining turgor causes the guard cells to close together, greatly reducing leaf water loss while also restricting entry of CO₂ for photosynthesis. Despite the anatomical simplicity of the stomatal valve, there is little consensus on how angiosperm stomata sense and respond to their extrinsic and intrinsic environment. Because stomata are the gatekeepers of terrestrial photosynthetic gas exchange, understanding their dynamic control is imperative for predicting CO₂

School of Plant Science, University of Tasmania, Private Bag 55, Hobart, Tasmania 7001, Australia.

*To whom correspondence should be addressed. E-mail: timothyb@utas.edu.au